Am J Transl Res 2019;11(7):4214-4231
www.ajtr.org /ISSN:1943-8141/AJTR0088678

Original Article

Combined therapy with atorvastatin and atorvastatin-pretreated mesenchymal stem cells enhances cardiac performance after acute myocardial infarction by activating SDF-1/CXCR4 axis

Xia-Qiu Tian[1,2], Yue-Jin Yang[1], Qing Li[1], Jun Xu[1], Pei-Sen Huang[1], Yu-Yan Xiong[1], Xiang-Dong Li[1], Chen Jin[1], Kang Qi[1], Lei-Pei Jiang[1], Gui-Hao Chen[1], Li Qian[3], Jiandong Liu[3], Yong-Jian Geng[4]

[1]State Key Laboratory of Cardiovascular Disease, Fuwai Hospital, National Center for Cardiovascular Diseases, Chinese Academy of Medical Sciences and Peking Union Medical College, Beijing 100037, People's Republic of China; [2]Center for Cardiac Intensive Care, Beijing Anzhen Hospital, Capital Medical University, Beijing Institute of Heart, Lung and Blood Vessel Diseases, Beijing 100029, People's Republic of China; [3]Department of Pathology and Laboratory Medicine, McAllister Heart Institute, University of North Carolina at Chapel Hill, Chapel Hill, North Carolina, 27599, United States; [4]The Center for Cardiovascular Biology and Atherosclerosis Research, Department of Internal Medicine, University of Texas Health Science Center at Houston, Houston 77030, Texas, United States

Received November 20, 2018; Accepted May 7, 2019; Epub July 15, 2019; Published July 30, 2019

Abstract: The SDF-1/CXCR4 signaling plays a critical role in the trafficking of mesenchymal stem cells (MSCs) to the sites of tissue damage. Our recent study demonstrated that atorvastatin (ATV) treatment improved the survival of MSCs, and ATV pretreated MSCs (^{ATV}MSCs) exhibited enhanced engraftment to injured myocardium. In this study, we investigated whether combined treatment with ATV and ^{ATV}MSCs enhances cardiac repair and regeneration by activating SDF-1/CXCR4 signaling in a rat model of acute myocardial infarction. Rats were randomized into eight groups: the Sham, AMI control and 6 other groups that were subjected to AMI followed by treatment with MSCs, ATV, ATV+MSCs, ^{ATV}MSCs, ATV+^{ATV}MSCs, ATV+^{ATV}MSCs+AMD3100 (SDF-1/CXCR4 antagonist), respectively. ATV+^{ATV}MSCs significantly potentiated targeted recruitment of MSCs to peri-infarct myocardium and resulted in further improvements in cardiac function and reduction in scar size compared with MSCs treatment alone at 4-week after AMI. More importantly, the cardioprotective effects conferred by ATV+^{ATV}MSCs were almost completely abolished by AMD3100 treatment. Together, our study demonstrated that ATV+^{ATV}MSCs significantly enhanced the targeted recruitment and survival of transplanted MSCs, and resulted in subsequent cardiac function improvement by augmenting SDF-1/CXCR4 signaling.

Keywords: Mesenchymal stem cells, atorvastatin, acute myocardial infarction, SDF-1/CXCR4

Introduction

Stem cell therapy has, for past two decades, emerged as one of the most promising therapeutic strategies to repair or regenerate post-infarct myocardium. Multiple preclinical studies have demonstrated beneficial effects of transplanted mesenchymal stem cells (MSCs) to attenuate adverse left ventricle remodeling [1-3]. MSCs are capable of conferring cardioprotective effects via multiple mechanisms [4, 5]. However, these beneficial effects observed in animal studies have not been fully translated to clinical benefits. Meta-analysis of randomized clinical trials indicated that cell therapy increased left-ventricular ejection fraction (LVEF) by just 3.17% in patients with acute myocardial infarction (AMI) [6] and 2.92% in patients with ischemic heart disease [7]. The low recruitment, poor survival and limited engraftment of transplanted MSCs in the ischemic environment are still the main hurdles that limit the therapeutic potential of MSCs [8, 9]. Developing strategies to promote MSCs recruitment and survival in ischemic myocardium is paramount to enhance the effectiveness of cell therapy for

myocardial infarction. The stromal cell-derived factor 1 (SDF-1) and its receptor CXC chemokine receptor 4 (CXCR4) have been demonstrated to play an essential role in the recruitment of stem cells to the ischemic myocardium [10-12]. However, SDF-1 expression is only transiently and slightly elevated in cardiac tissues following ischemic insult [12]. Therefore, inducing SDF-1 expression and promoting the activation of SDF-1/CXCR4 signaling may be pivotal for improving MSCs therapeutic efficiency [13, 14].

Our previous studies demonstrated statins, a type of clinically widely used lipid-lowering drug, could improve the survival and therapeutic effect of MSCs in murine and porcine models of AMI via multiple mechanisms [15-17]. Atorvastatin (ATV) was also reported to enhance SDF-1 expression in the injured myocardium in a rat model of AMI [18], CXCR4 expression in endothelial progenitor cells [19], and promote the migration of adipose-derived MSCs through SDF-1/CXCR4 pathway in a rat model of ischemia-reperfusion injury [20]. Additionally, our recent studies showed that ATV pretreatment of MSCs (^{ATV}MSCs) not only protected these cells from apoptosis, but also increased the expression of CXCR4 on the surface of MSCs [21, 22]. In this study, we sought to determine the therapeutic effect of combined oral administration of ATV with ^{ATV}MSCs transplantation (ATV+^{ATV}MSCs) in a rat model of AMI. We found that ATV+^{ATV}MSCs markedly enhanced targeted recruitment, retention and survival of the transplanted MSCs. ATV+^{ATV}MSCs also led to significantly enhanced improvement in heart function, further attenuation of ventricular structural remodeling and marked reduction in infarct size. Mechanistically, we revealed that the improved cardioprotective effects of ATV+^{ATV}MSCs were mostly associated with an augmented activation of SDF-1/CXCR4 signaling. These findings demonstrated that ATV combined with ^{ATV}MSCs might hold potential for future clinical applications.

Materials and methods

Animals

All experimental protocols were approved by the Care of Experimental Animals Committee of Fuwai Hospital and conformed to the Guide for the Care and Use of Laboratory Animals (NIH Publication No. 85-23, revised 1996).

Male Sprague-Dawley rats (60-80 g) were used as the donors of MSCs, while female rats (200-220 g) as the recipients and AMI models. In the first set of experiments, 55 female rats were randomized into 3 groups: sham operation group (Sham) (n = 15), AMI control (Control) (n = 20), and ATV oral administration (ATV) (n = 20). The ATV group received ATV (Pfizer Pharmaceutical Company) (10 mg/kg/d) by gavage once a day, starting from 2 hours after AMI.

In the second set of experiments, a total of 115 female rats were randomly divided into 8 groups: sham operation (Sham) (n = 15), AMI control (AMI) (n = 15), oral administration of ATV group (ATV) at 10 mg/kg/d (n = 15), MSCs transplantation (MSCs) (n = 15), ATV oral administration in combination with MSCs transplantation (ATV+MSCs) (n = 15), ATV-pretreated MSCs group (^{ATV}MSCs), ATV oral administration combined with ^{ATV}MSCs transplantation (ATV+^{ATV}MSCs) (n = 15), and ATV+^{ATV}MSCs+AMD-3100 (SDF-1/CXCR4 antagonist) (n = 15). In the MSCs group, 2×10^6 CM-DiI labeled MSCs were transplanted intravenously at 1-week after AMI. In the ATV group, high dose of ATV (10 mg/kg/d) was given to the rats by gavage every day from 2 hours after the establishment of AMI model for 4 weeks. In the ATV+MSCs group, both ATV and MSCs were administered as described above. In the ^{ATV}MSCs group, the MSCs were co-cultured with 1 μM ATV for 24 hours before transplantation intravenously at 1-week post AMI. In the ATV+^{ATV}MSCs group, the rats were given both intragastric administration of ATV once a day for 4 weeks and intravenously infusion of ^{ATV}MSCs at 1-week post AMI. In the ATV+^{ATV}MSCs+AMD3100 group, the SDF-1/CXCR4 antagonist AMD3100 (Sigma, St. Louis, MO, A5602) (5 mg/kg/d) was intraperitoneally injected once a day from 2 hours post AMI in addition to the administration of ATV and ^{ATV}MSCs as mentioned above.

Bone marrow mesenchymal stem cells isolation, culture and delivery

Briefly, bone marrow was harvested from the tibia and femur of Sprague-Dawley rats (60-80 g, male) and plated into cell culture flasks with complete medium containing Iscove's Modified Dulbecco's Medium (IMDM, Gibco, USA), 10% fetal bovine serum (Gibco, USA) and 1% penicillin-streptomycin (Gibco, USA) at 37°C. When

the cell cultures reached 80% confluence, they were detached using 0.25% trypsin-EDTA (Gibco, USA) and subcultured at the ratio of 1:3. All the cells used in the experiments were at passage 3.

Prior to transplantation, MSCs were labeled with Cell Tracker CM-DiI (Molecular Probe, Invitrogen, USA). The ATV pretreated-MSCs were incubated with 1 μM ATV for 24 h before transplantation. 2.0×10^6 CM-DiI-labeled MSCs or CM-DiI-labeled ATV pretreated-MSCs in a total volume of 0.5 ml phosphate-buffered saline (PBS) were injected through the tail vein at 1-week post AMI. The control group received the same volume of cell-free PBS.

Establishment of acute myocardial infarction model

The AMI rat model was established as previously described [17]. Briefly, permanent ligation of the proximal left anterior descending coronary artery (LAD) was conducted with a 6-0 polyester suture 1-2 mm from the tip of the left atrial appendage. Successful ligation of the LAD was verified by myocardial blanching and observation of abnormal movement of the anterior wall. The sham-operation group received the same procedure except for coronary ligation.

Immunohistochemistry

For the rats used in the first set of experiments, the heart tissues were harvested and fixed after sacrificed at day 1, day 7 and day 14 post AMI. Paraffin sections were cut at 5 μm thickness, and mounted on glass slides for staining. Slides were deparaffinized by gradient ethanol solution, and subjected to antigen retrieval in hot citric acid buffer. After cooling, slides were permeabilized with 0.2% Triton-100 for 15 minutes and were blocked with 1% BSA in PBS for 2 hours. Then, the slides were incubated overnight with primary rabbit anti-SDF-1 antibody (1:100, Santa Cruz, USA) in 4°C followed by incubation with the goat anti-rabbit IgG (Beyotime, China) secondary antibody and color reaction with the DAB kit. In every section, 4 high-power fields in peri-infarct region were selected randomly. The mean optical density values of SDF-1-positive regions were analyzed using Zeiss software.

RT-PCR and ELISA

RT-PCR and ELISA were performed to analyze expression of SDF-1 mRNA and proteins, respectively. Quantitative immunoassay was used for evaluating expression of SDF-1 in peri-infarct area of myocardium at day 1, day 7 and day 14 after AMI according to manufacturer's protocol (Abnova, Taiwan). Tissues from the peri-infarct regions of myocardium or the supernatant of the culture medium were homogenized. Protein concentrations were adjusted to 10 mg/ml. Recombinant rat SDF-1 supplied by the kit was used to plot standard curve. Optical density of each sample was detected by Enzyme-labeling measuring instrument at the wavelength of 450 nm, and the concentration was determined on the standard curve. All the measurements were repeated for 3 times to obtain arithmetic average.

Real time PCR was performed to analyze the expression of SDF-1 mRNA. Total RNA was extracted from heart tissues via Trizol reagent (Invitrogen, USA), per manufacturer's instructions. cDNA was synthesized from the total RNA using TIANScript RT Kit (Qiagen, German). Real time PCR was performed with SYBR FAST qPCR Kit Master Mix (2 ×) Universal (KAPA, USA). β-actin was used as housekeeping gene for normalization. The reaction conditions were as follows: 95°C for 3 min, followed by 40 cycles of 95°C for 3 s, and 63°C for 20 s. The sequences of primers ultimately used were SDF-1-F, 5'-GCATCAGTGACGGTAAGC; SDF-1-R, 5'-AAGGGCACAGTTTGGAGT; β-actin-F, 5'-GCACCATGAAGATCAAGATCATT; β-actin-R, 5'-TAACAGTCCGCCTAGAAGCATT. Data were normalized via standard comparative CT method.

Fluorescence microscopy

Hearts were embedded in Tissue-Tek OCT compound (Sakura) and cut into 5 mm-thick serial sections, and nuclei were stained with DAPI. The sections were analyzed using a laser scanning confocal microscope (Leica, Germany). The excitation wavelengths were 561 nm and 405 nm for detection of CM-DiI and DAPI. The number of labeled MSCs was quantified by a blinded researcher in 10 randomized high-power fields (× 600) per animal. Immunofluorescence staining was performed to evaluate vessel density, c-Kit$^+$ cells in peri-infarct areas and the differentiation of MSCs. Sections were fixed

in 4% paraformaldehyde rinsed with PBS, and blocked with 0.1% PBS-T containing 1% BSA. After incubation with primary antibodies at 4°C overnight, sections were washed with PBS, and co-incubated with goat anti-rabbit (1:500, Cell Signaling Technology, Danvers, MA) and goat anti-mouse Alexa Fluor 488 secondary antibody (1:100, R&D systems, Minneapolis, MN, NL007). After washing, the nuclei were counterstained with DAPI (Invitrogen). The sections were analyzed under a laser scanning confocal microscope FV1000 (Olympus) and 4 random high-power fields were chosen per animal. The primary antibodies used in this study were as follows: rabbit anti-CD31 (1:300, Abcam, Cambridge, MA), rabbit anti-α-SMA (1:50, Abcam, Cambridge, MA), mouse anti-c-Kit (1:50, Abcam, Cambridge, MA), and mouse anti-c-TnT (1:100, Abcam, Cambridge, MA).

Echocardiography and catheterization

Transthoracic echocardiography was performed at 1-week (baseline) and 4-week (endpoint) after AMI with a 12-MHz phased-array transducer (Sonos 7500, Phillips). After two-dimensional images were obtained, the left ventricular end-systolic diameter (LVESd) and end-diastolic diameter (LVEDd) were measured under M-mode tracings from the parasternal long axis view at the papillary muscle level. Left ventricular fractional shortening (LVFS) and left ventricular ejection fraction (LVEF) were calculated using the follows equations: LVFS (%) = (LVEDd - LVESd)/LVEDd × 100%, and LVEF (%) = $(LVEDd)^3$ - $(LVESd)^3$]/$(LVEDd)^3$ × 100%. Measurements performed over three consecutive heart cycles were averaged.

Left heart catheterization was also performed at 4-week after AMI to assess cardiac function. Briefly, a catheter filled with heparin solution was inserted into left ventricle through the right common carotid artery. The left ventricular pressure curve was recorded, and the data of the left ventricular end-diastolic pressure (LVEDP), as well as the left ventricular pressure maximal rate of rise and fall (± dp/dt_{max}) were recorded.

Assessment of infarct size and inflammation

At 4-week post AMI, the animals were sacrificed to collect heart tissues. The hearts were fixed in 10% formalin and embedded in paraffin. The paraffin sections were stained with Masson's trichrome and Hematoxylin-Eosin (H&E). For Masson's trichrome staining, the blue area was regarded as fibrotic tissue and taken as the infarct size. Five different ventricular slices from each heart were scanned and computerized with the Image-Pro-Plus software. The infarct size, i.e. fibrotic area, was expressed as percentages of the total left ventricular areas (fibrotic area/total left ventricular area × 100%). The densities of neutrophils in the peri-infarct myocardium were determined from 10 randomly selected areas in a blinded fashion based on morphology of nuclei and cell size, as described previously [23].

Heart homogenates were prepared, and commercially available quantitative proteomics kits (Ray Biotech, Atlanta, USA) were used to measure the IL-1β, IL-6, TNF-α and IL-10 level in different groups. Optical density of each sample was detected by Enzyme-labeling measuring instrument at a wavelength of 532 nm, and the concentration was figured out on the standard curve.

TUNEL assay

Cell apoptosis was determined by TdT-mediated dUTP nick-end labeling (TUNEL) using the In Situ Cell Death Detection kit (Roche, Mannheim, Germany, 11772465001) according to the manufacture's instruction. TUNEL-positive cells were examined under fluorescence microscope at 200 × magnification in 5 randomly selected fields. Nuclei were stained with DAPI in blue while apoptotic nuclei were green in color. The results were presented as the percentage of apoptotic cells/total cells.

Western blot analysis

Tissues were extracted from infarcted and peri-infarct regions of the myocardium. Protein concentrations were measured with BCA assay. To detect the expression of Bcl-2 and Bax in the heart tissue, 50 mg of protein lysate was resolved by SDS-PAGE, transferred to nitrocellulose membranes (Life Technologies), and blocked with 5% non-fat dry milk. The primary antibodies used were as follows: β-actin (1:1000, Cell Signaling Technology, Danvers, MA), Bcl-2 (1:1000, Cell Signaling Technology, Danvers, MA) and Bax (1:500, Cell Signaling Technology, Danvers, MA). Target protein sig-

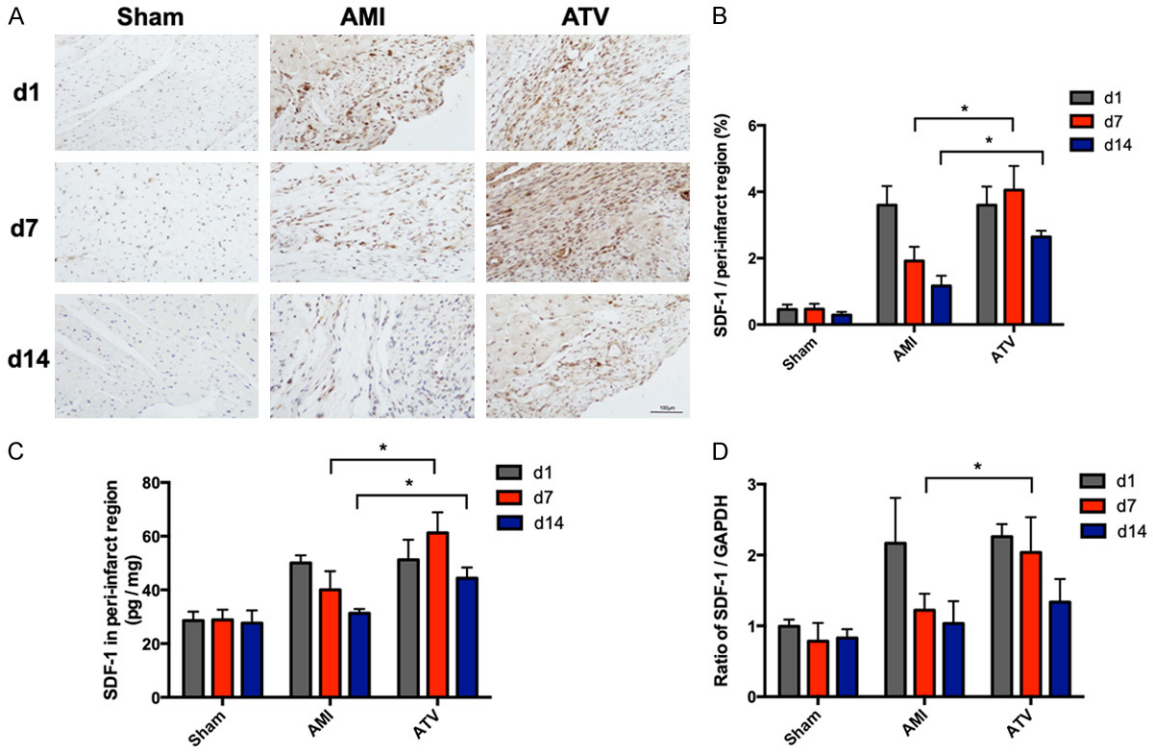

Figure 1. The time course changes of SDF-1 expression in peri-infarct myocardium after AMI. A, B. Representative images and quantitative data of SDF-1 immunohistostaining in different groups at day 1, day 7 and day 14 post AMI (× 200). SDF-1 expression in the infarcted myocardium was significantly elevated at 1 day after AMI compared with Sham group, and followed by rapid decline within 1 week. In the ATV group, SDF-1 maintained its peak level at day 7, and exhibited significant increased level at day 14 post AMI compared with the AMI group. C. ELISA assessment of SDF-1 expression during the time course. The expression of SDF-1 in ATV group were significantly elevated at day 7 and day 14 compared with AMI group. D. Assessment of mRNA expression of SDF-1 with RT-PCR. The mRNA expressions of SDF-1 in ATV group were significantly elevated at day 7 compared with AMI group. n = 5 for each group. *P<0.05 between groups. AMI: acute myocardial infarction; ATV: atorvastatin; MSCs: mesenchymal stem cells; SDF-1: stromal cell-derived factor-1. Scale bar = 100 μm.

nals were normalized to β-actin as a loading control (1:1000, Zhongshan Jinqiao, China). After washing, the membranes were incubated for 1 h at room temperature in blocking solution containing the peroxidase-conjugated secondary antibodies. Next, the membranes were washed and processed for analysis using a Chemiluminescence Detection Kit (Pierce) according to the manufacturer's instructions. Densitometry analysis was completed using Quantity One software.

Statistics analysis

All continuous variables were expressed as mean ± SD, and analyses were performed with GraphPad Prism software (Version 6.0c, GraphPad Software, La Jolla, CA). Statistical significance among groups was evaluated with One Way ANOVA followed by post hoc LSD-test, and a value of P<0.05 was considered statistically significant.

Results

ATV enhances SDF-1 expression in the heart with AMI

Previous studies showed that SDF-1 and its receptor CXCR4 play an essential role in the recruitment of stem cells to ischemic myocardium, but a detailed analysis of their expression in an infarcted heart is lacking. We determined SDF-1 expression in a rat model of AMI. Both immunohistochemistry (**Figure 1A**, **1B** and Table S1) and ELISA analyses (**Figure 1C**) showed that SDF-1 expression in the peri-infarct myocardium was significantly elevated compared with that in the Sham group. In the peri-infarct region, SDF-1 expression peaked at

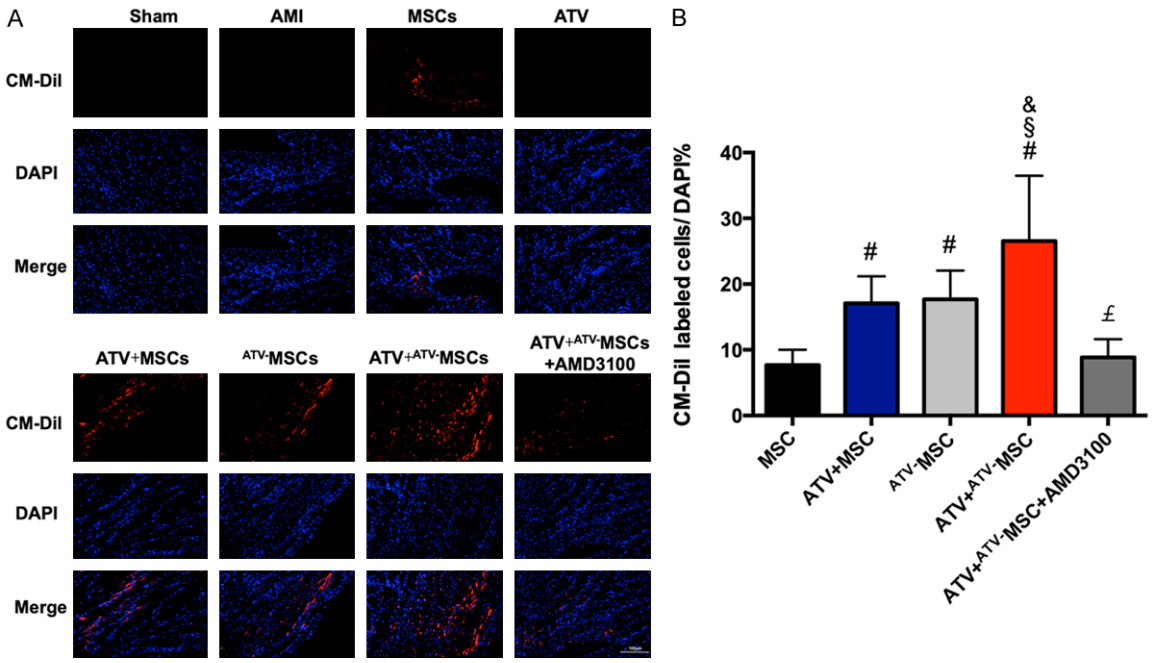

Figure 2. Engraftment of transplanted MSCs labeled with CM-DiI. A. Engraftment of CM-DiI-labeled cells in the peri-infarct myocardium at the end of 4 weeks post AMI (× 600). B. Quantitation of CM-DiI-labeled cells in the peri-infarct myocardium per high power field (HPF) in each group. The number of CM-DiI positive cells in the ATV+MSCs and ^{ATV}MSCs groups was both markedly higher than that in the MSCs-only group. The ATV+^{ATV}MSCs group demonstrated the highest number of CM-DiI positive cells in the heart among all groups, which was significantly decreased with the treatment of AMD3100. n = 10 in each group. #P<0.05 compared with MSCs group; §P<0.05 compared with ATV+MSCs group; &P<0.05 compared with ^{ATV}MSCs group; £P<0.05 compared with ATV+^{ATV}MSCs group. AMI: acute myocardial infarction; ATV: atorvastatin; MSCs: mesenchymal stem cells; ^{ATV}MSCs: atorvastatin pretreated mesenchymal stem cells; CM-DiI: 1,1'-dioctadecyl-3,3,3',3'-tetramethylindocarbocyanine perchlorate; DAPI: 4'6-diamidino-2-phenylindole dihydrochloride. Scale bar = 100 μm.

day 1 post AMI followed by rapid decline within 1 week. Interestingly, high dose of oral ATV administration significantly extended the window of SDF-1 upregulation. In the ATV group, SDF-1 maintained its peak level of expression for about 1 week (P<0.05), and also exhibited significant increased level of expression in the second week post AMI (P<0.05) compared with that in the AMI group. This observation was further confirmed by qRT-PCR analysis (**Figure 1D**). The extended window of *SDF-1* upregulation provided us greater flexibility for MSCs delivery, and we hypothesized that delivering MSCs at post-AMI inflammatory stage could enhance MSCs survival and targeted recruitment. Accordingly, in this study, we opted to deliver MSCs at 1-week post AMI.

Combined therapy of ATV and ^{ATV}MSCs enhances the recruitment and survival of MSCs in the peri-infarct myocardium

The recruitment and retention rates of transplanted MSCs in the peri-infarct myocardium were investigated at 4-week after infarction. While the number of CM-DiI positive cells in the ATV+MSCs and ^{ATV}MSCs groups was both markedly higher than that in the MSCs-only group (17.09% and 17.67% vs. 7.7%, P<0.05), the ATV+^{ATV}MSCs group demonstrated the highest number of CM-DiI positive cells in the heart among all groups (26.54% vs. 7.7%, P<0.05). Together, these data indicated that ATV treatment, especially the combination regimen (ATV+^{ATV}MSCs), remarkably augmented targeted recruitment and survival of transplanted MSCs (**Figure 2A**, **2B**).

Combined therapy of ATV and ^{ATV}MSCs improves cardiac function and inhibits adverse ventricular remodeling

At baseline, the AMI rats that were randomly allocated to different groups did not exhibit any differences in cardiac structure and cardiac function (**Table 1**; **Figure 3A** and **3B**), validating the reliability and consistency of the established AMI models. At 4-week post AMI, the

Table 1. Cardiac function determined by echocardiography at baseline and endpoint

		LVEF (%)	LVFS (%)	LVEDd (mm)	LVESd (mm)
Sham	Baseline	82.53±3.82	44.55±4.20	6.61±0.30	3.66±0.2
	Endpoint	82.56±1.74	44.41±1.91	6.40±0.36	3.56±0.15
	Changes	0.03±3.08	-0.14±3.28	-0.21±0.25	-0.10±0.24
AMI	Baseline	51.25±3.09	21.46±1.69	6.72±0.38	5.27±0.23
	Endpoint	45.70±3.18	19.29±1.70	8.51±0.45	6.86±0.35
	Changes	-5.55±2.52	-2.17±1.56	1.79±0.54	1.59±0.46
MSCs	Baseline	50.88±1.56	21.24±1.15	6.43±0.36	5.07±0.32
	Endpoint	56.45±2.12	24.73±1.63	8.34±0.31	6.28±0.33
	Changes	5.58±3.13*	3.49±2.14*	1.91±0.63$^{\$}$	1.21±0.61$^{\$}$
ATV	Baseline	50.60±3.41	21.13±2.16	6.94±0.40	5.47±0.33
	Endpoint	56.59±1.83	24.98±1.46	8.17±0.32	6.13±0.31
	Changes	5.99±3.98*	3.85±2.11*	1.23±0.59$^{\#}$	0.66±0.51$^{*,\#}$
ATV+MSCs	Baseline	51.71±2.53	21.57±1.39	6.87±0.23	5.39±0.25
	Endpoint	64.5±1.90	29.77±1.81	7.85±0.22	5.51±0.16
	Changes	12.79±2.11$^{*,\#,\$}$	8.20±1.76$^{*,\#,\$}$	0.98±0.30$^{*,\#,\$}$	0.12±0.22$^{*,\#}$
^{ATV}MSCs	Baseline	52.24±1.23	21.84±0.67	6.82±0.22	5.33±0.19
	Endpoint	63.13±1.29	28.67±1.40	7.60±0.35	5.42±0.24
	Changes	10.89±1.66$^{*,\#,\$}$	6.84±1.54$^{*,\#,\$}$	0.77±0.38$^{*,\#,\$}$	0.08±0.30$^{*,\#,\$}$
ATV+^{ATV}MSCs	Baseline	51.17±2.58	21.41±1.43	6.78±0.21	5.33±0.21
	Endpoint	67.01±1.38	31.27±1.21	7.48±0.19	5.14±0.13
	Changes	15.84±2.85$^{*,\#,\$,\&}$	9.86±1.54$^{*,\#,\$,\&}$	0.70±0.29$^{*,\#,\$}$	-0.19±0.24$^{*,\#,\$}$
ATV+^{ATV}MSCs+AMD3100	Baseline	52.51±2.13	22.13±1.31	6.65±0.27	5.18±0.22
	Endpoint	54.22±1.67	23.29±0.88	8.65±0.28	6.63±0.23
	Changes	1.71±2.47$^{*,\$,\&,£}$	1.15±1.57$^{*,\&,£}$	2.00±0.45$^{\$,\&,£}$	1.46±0.38$^{\$,\&,£}$

ATV: atorvastatin; MSCs: mesenchymal stem cells; ^{ATV}MSCs: atorvastatin pretreated mesenchymal stem cells; AMI: acute myocardial infarction; LVEF: left ventricular ejection fraction; LVFS: left ventricular fractional shortening; LVEDd: left ventricular end-diastolic dimension; LVESd: left ventricular end-systolic dimension. n = 10 for each group. $^{*}P$<0.05 compared with AMI group; $^{\#}P$<0.05 compared with MSCs group; $^{\$}P$<0.05 compared with ATV group; $^{\&}P$<0.05 compared with ^{ATV}MSCs group; $^{£}P$<0.05 compared with ATV+^{ATV}MSCs group.

MSCs-only group demonstrated significantly enhanced value of change in LVEF (ΔLVEF) and LVFS (ΔLVFS) (P<0.05) compared with the AMI control group. While the enhancement in LVEF and LVFS by both ATV+MSCs and ^{ATV}MSCs treatments reached statistic significant (P< 0.05), the combination regimen (ATV+^{ATV}MSCs) demonstrated a much more significant improvement in LVEF (P<0.05, 15.84% vs. 5.58% by MSCs treatment) and LVFS (P<0.05, 9.86% vs. 3.49% by MSCs treatment), respectively compared with MSCs-only treatment. Likewise, the values of change in LVEDd (ΔLVEDd) and LVESd (ΔLVESd) were all dramatically reduced in ATV+MSCs, ^{ATV}MSCs and ATV+^{ATV}MSCs groups compared with those in the MSCs-only group (P<0.05). However, we did not observe any significant differences in the values of change in LVEDd and LVESd between MSCs-only and AMI control groups (P>0.05), and among the groups of ATV+MSCs, ^{ATV}MSCs, and the ATV and ^{ATV}MSCs combination (P>0.05) (**Figure 3B**). Altogether, these data indicated that the combination regimen demonstrated significant more potent therapeutic effect in enhancing cardiac function and attenuation of adverse ventricular structural remodeling.

We also performed left heart catheterization at 4-week post AMI to further assess heart function (Table S2; Figure S1). Compared with AMI group, both MSCs- and ATV-only groups had significantly decreased LVEDP (P<0.05). Consistent with the LVEF and LVFS data, the animals in the ATV+MSCs and ^{ATV}MSCs groups exhibited further decreased LVEDP (P<0.05) compared with those in the MSCs-only group. More importantly, the ATV+^{ATV}MSCs group out-

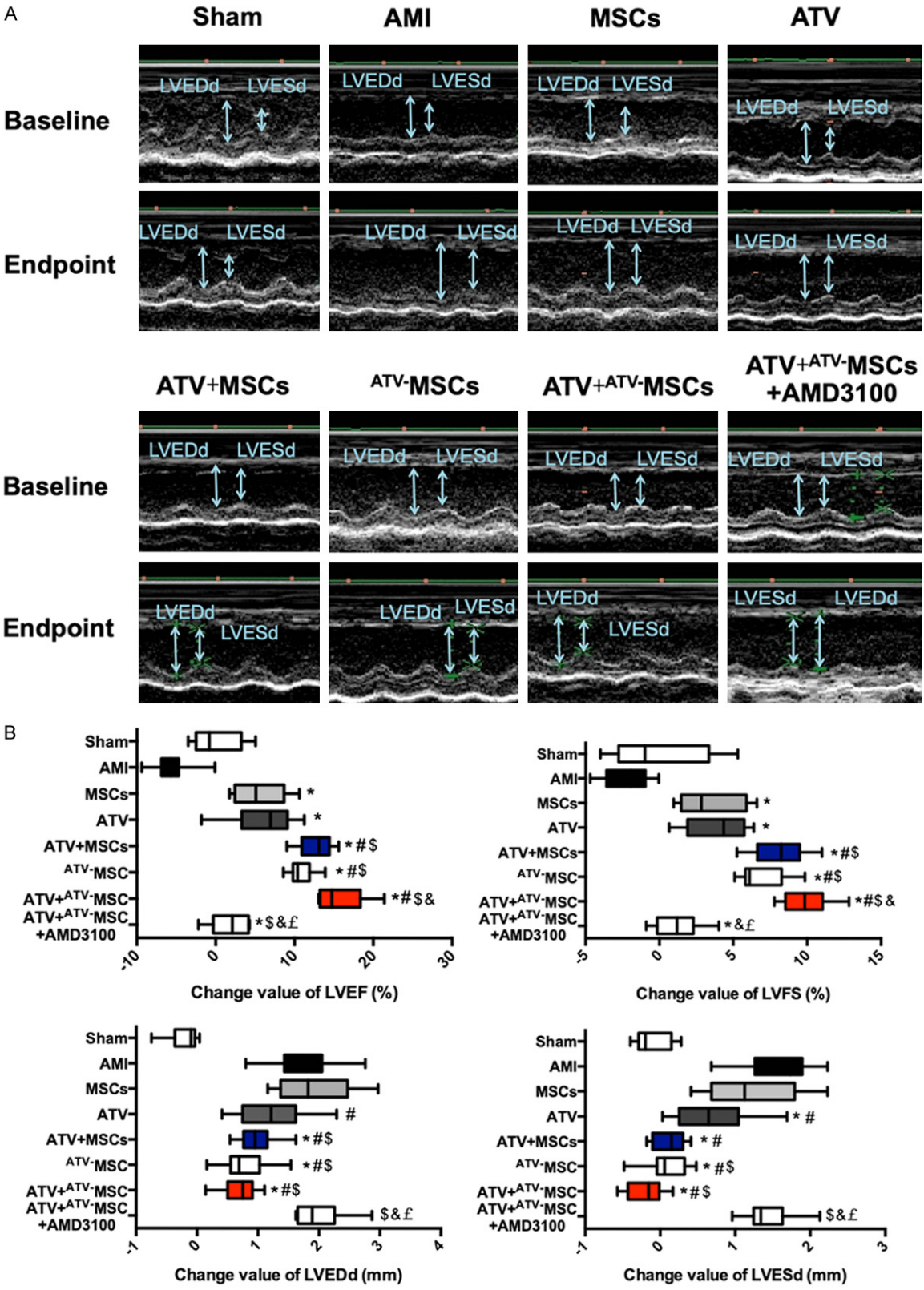

Figure 3. Cardiac function assessment with echocardiography. A. Representative images of M-mode echocardiography at baseline (1-week post AMI) and endpoint (4-week post AMI). B. The change values (to endpoint from baseline) of LVEF, LVFS, LVEDd and LVESd. At the baseline, the LVEF, LVFS, LVEDd and LVESd did not differ between AMI rats in different groups. At the endpoint, the combination regimen (ATV+$^{ATV-}$MSCs) demonstrated a most sig-

nificant improvement in LVEF and LVFS, which was significantly abrogated with the treatment of AMD3100. The values of change in LVEDd (ΔLVEDd) and LVESd (ΔLVESd) were all dramatically reduced in ATV+MSCs, ^{ATV}MSCs and ATV+^{ATV}MSCs groups compared with those in MSCs-only group. Compared with ATV+^{ATV}MSCs group, the addition administration of AMD3100 significantly increased values of change in LVEDd and LVESd. *P<0.05 compared with AMI group; #P<0.05 compared with MSCs group; $$P$<0.05 compared with ATV group; &P<0.05 compared with ^{ATV}MSCs group; £P<0.05 compared with ATV+^{ATV}MSCs group. AMI: acute myocardial infarction; ATV: atorvastatin; MSCs: mesenchymal stem cells; ^{ATV}MSCs: atorvastatin pretreated mesenchymal stem cells; LVEF: left ventricular ejection fraction; LVFS: left ventricular fractional shortening; LVEDd: left ventricular end-diastolic dimension; LVESd: left ventricular end-systolic dimension.

performed all other groups, and the combination regimen remarkably reduced LVEDP compared with ATV+MSCs and ^{ATV}MSCs treatments (10.61 mmHg vs. 14.69 mmHg and 17.46 mmHg, P<0.05). Concomitantly, the dp/dt in both ATV+MSCs and ^{ATV}MSCs groups was significantly increased compared with MSCs- or ATV-alone group (P<0.05), and further significantly enhanced in ATV+^{ATV}MSCs group compared with the former two groups (P<0.05). These results suggested that ATV+^{ATV}MSCs is the most effective treatment that promotes the functional recovery of infarcted hearts.

Combined therapy of ATV and ^{ATV}MSCs reduces infarct size and inflammation

We performed histological analysis at 4-week after cell transplantation. Masson's trichrome staining showed that transmural infarction existed in all experimental groups, while the infarct size in ATV and MSCs treated AMI rats were both reduced compared with that in the AMI controls (P<0.05). The infarct size in the ATV+MSCs and ^{ATV}MSCs groups was also significantly reduced (P<0.05) compared with that in the ATV- and MSCs-alone groups. Compared with all other group, the ATV+^{ATV}MSCs group had the smallest infarct size, which was further remarkably reduced compared with those in the MSCs and ^{ATV}MSCs groups (16.06% vs. 27.90% and 20.28%, P<0.05), and was comparable to that in the ATV+MSCs group (**Figure 4A**, **4B**).

Myocardial infarction triggers intense inflammatory response. H&E staining demonstrated massive infiltration of inflammatory cells as indicated by an increased number of neutrophils per mm^2 in the peri-infarct regions of myocardium in the AMI group. However, inflammatory cell infiltration was significantly reduced in the ATV or MSCs alone groups. Further significant reduction in inflammatory cell infiltration was observed in both ATV+MSCs and ^{ATV}MSCs groups, while the ATV+^{ATV}MSCs group exhibited the most significant reduction in inflammatory cell infiltration (P<0.05) (**Figure 4C**, **4D**).

To further assess the inflammatory response, we measured the levels of inflammatory cytokines in the peri-infarct region of myocardial tissues by protein microarray. As shown in **Figure 4E** and Table S3, administration of MSCs or ATV effectively reduced the expression level of pro-inflammatory cytokines IL-1β, IL-6 and TNF-α in myocardial tissue (P<0.05). Compared with MSC-only group, ATV+MSCs or ^{ATV}MSCs group had significantly reduced level of IL-1β, IL-6 and TNF-α (P<0.05). In the ATV+^{ATV}MSCs group, the expression of IL-1β and IL-6 but not TNF-α further decreased to a significantly lower level (P<0.05). Compared with the AMI group, the level of anti-inflammatory cytokine IL-10 was significantly higher only in the ATV+^{ATV}MSCs group (P<0.05). In sum, our data indicated that ATV+^{ATV}MSCs exerted potent anti-inflammation effect and was the most effective anti-inflammatory treatment.

Combined therapy of ATV and ^{ATV}MSCs inhibits cardiomyocytes apoptosis in the peri-infarct region

TUNEL staining was performed to evaluate the anti-apoptotic effects of MSCs and ATV on AMI-induced cardiomyocytes apoptosis. As shown in **Figure 5A** and **5B**, AMI-induced cardiomyocytes apoptosis was significantly reduced by both MSCs and ATV treatments. ATV+MSCs and ^{ATV}MSCs also significantly reduced cardiomyocytes apoptosis in the peri-infarct myocardium (P<0.05), with the former treatment being more effective than the latter one (P<0.05). ATV+^{ATV}MSCs exerted more potent anti-apoptotic effect compared with MSCs only (6.57% vs. 25.3%, P<0.05), ATV+MSCs, and ^{ATV}MSCs (P<0.05). We then performed western blot analysis to assess the expression of Bcl-2 and Bax in peri-infarct myocardium. As shown in

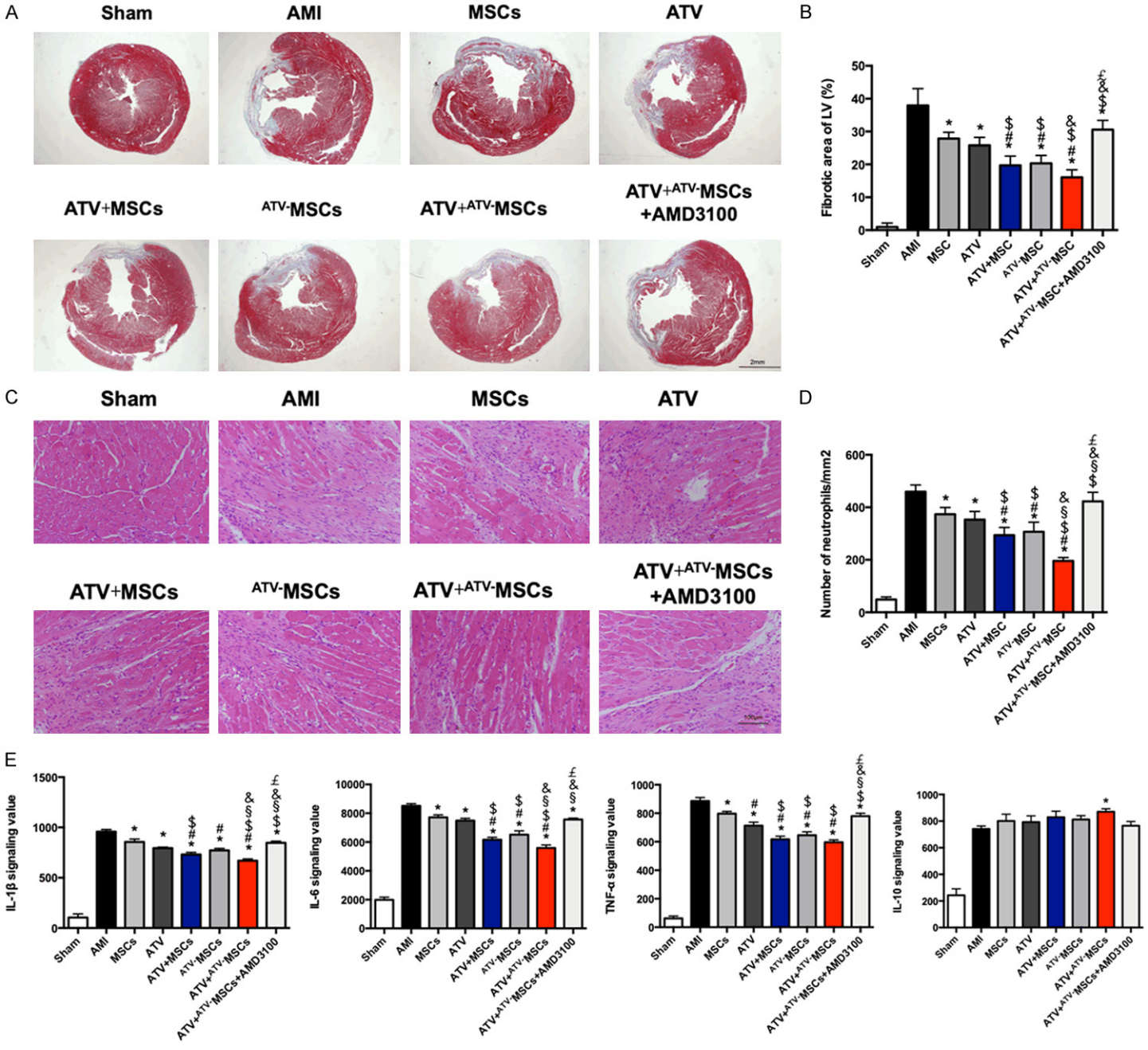
A
Sham
AMI
MSCs
ATV
ATV+MSCs
ATV-MSCs
ATV+ATV-MSCs
ATV+ATV-MSCs +AMD3100
B
Fibrotic area of LV (%)
C
D
Number of neutrophils/mm2
E
IL-1β signaling value
IL-6 signaling value
TNF-α signaling value
IL-10 signaling value

Figure 4. Infarct size was measured using Masson's trichrome staining. Inflammation was measured using Hematoxylin-Eosin staining and cytokine measurement. (A) Representative images of Masson's trichrome staining in each group. (B) Quantitative data for the left ventricular infarct size. Compared to all other group, the ATV+$^{ATV-}$MSCs group had the smallest infarct size, which was significantly reversed with the treatment of AMD3100. (C) Representative images of Hematoxylin-Eosin staining in each group (× 200). (D) Quantitative data for the infiltration of neutrophils in peri-infarct myocardium. The ATV+$^{ATV-}$MSCs group exhibited the most reduced neutrophils infiltration, which was significantly abolished with the treatment of AMD3100. (E) Expressions of IL-1β, IL-6, TNF-α, IL-10 in the peri-infarct myocardium in each group. In the ATV+$^{ATV-}$MSCs group, the expression of IL-1β and IL-6 but not TNF-α further decreased to a significantly lower levels, which was reversed with the treatment of AMD3100. Compared with the AMI group, the level of anti-inflammatory cytokine IL-10 was significantly higher only in the ATV+$^{ATV-}$MSCs group. n = 10 in each group. *P<0.05 compared with AMI group; #P<0.05 compared with MSCs group; $$P$<0.05 compared with ATV group; §P<0.05 compared with ATV+MSCs group; &P<0.05 compared with $^{ATV-}$MSCs group; £P<0.05 compared with ATV+$^{ATV-}$MSCs group. AMI: acute myocardial infarction; ATV: atorvastatin; MSCs: mesenchymal stem cells; $^{ATV-}$MSCs: atorvastatin pretreated mesenchymal stem cells; IL: interleukin; TNF: tumor necrosis factor. Scale bar = 2 mm (A), 100 μm (C).

Figure 5C-E, both MSCs and ATV treatment slightly increased Bcl-2 expression (P>0.05). Notably, ATV+$^{ATV-}$MSCs treatment significantly increased Bcl-2 expression compared with MSCs- and ATV-only groups (P<0.05). In contrast, Bax expression was reduced in both ATV and ATV+MSCs treatment groups compared with AMI control (P<0.05), which further decreased in the $^{ATV-}$MSCs and ATV+$^{ATV-}$MSCs groups (P<0.05).

Combined regimen of ATV and $^{ATV-}$MSCs promotes angiogenesis and c-Kit$^+$ cell infiltration in peri-infarct myocardium

We performed antibody staining against endothelial cell marker CD31 and smooth muscle cell marker α-smooth-muscle actin (α-SMA) at 4-week after AMI to assess angiogenesis and arteriogenesis in peri-infarct myocardium, respectively. As shown in **Figures 6A**, **6B**, S2; Table S4, the number of both CD31 and α-SMA positive vessels in MSCs group were significantly higher than that in the AMI control group (P<0.05). Both arteriogenesis and angiogenesis were also significantly increased in the ATV+MSCs and $^{ATV-}$MSCs groups (P<0.05) compared with MSCs or ATV treatment groups. Of particular note, ATV+$^{ATV-}$MSCs group demonstrated further significantly enhanced arteriogenesis and angiogenesis compared with $^{ATV-}$MSCs (SMA$^+$: 15.0 vs. 11.2, P<0.05; CD31$^+$: 39.8 vs. 22.8, P<0.05) and ATV+MSCs groups (CD31$^+$: 39.8 vs. 22.8; P<0.05).

We counted the number of c-Kit$^+$ cells in the peri-infarct myocardium using immunofluorescence staining (**Figure 6C**, **6D**). Compared with that in the AMI control group, the number of c-Kit$^+$ cells in MSCs, ATV+MSCs and $^{ATV-}$MSCs groups all had a significant increase (P<0.05) in the border zone near the infarct area (**Figure 6C**, **6D**; Table S4). We also noticed that the ATV+MSCs group had significantly more c-Kit$^+$ cells than the MSCs group (P<0.05), while the ATV+$^{ATV-}$MSCs group demonstrated a marked increase in the number of c-Kit$^+$ cells compared with all other groups (17.0% vs. 7.2%, 10.8% and 10.2%, P<0.05), suggesting that ATV+$^{ATV-}$MSCs had the strongest effect to mobilize c-Kit$^+$ cells (P<0.05). Of particular note, we found that the CM-DiI-positive cells were rarely positive for cTnT staining in all groups, indicating that MSCs, ATV+MSCs, even ATV+$^{ATV-}$MSCs did not enhance the trans-differentiation of the transplanted MSCs into cardiomyocytes in the post-infarction hearts (Figure S3). Collectively, these observations suggest that ATV+$^{ATV-}$MSCs can promote angiogenesis with rare trans-differentiation of MSCs into cardiomyocytes in peri-infarct region.

Combined therapy with ATV and $^{ATV-}$MSCs exerts cardioprotective effects by activating the SDF-1/CXCR4 axis

To investigate the mechanism by which ATV+$^{ATV-}$MSCs exerts the aforementioned cardioprotective effects, we used AMD3100, an inhibitor of SDF-1/CXCR4 signaling, in addition to ATV+$^{ATV-}$MSCs treatment. Notably, the cardioprotective effects of the ATV+$^{ATV-}$MSCs combination regimen were almost completely abolished by the treatment of AMD3100, as indicated by the predominantly decreased LVEF, LVFS and ± dp/dt, increased LVEDP, LVEDd, LVESd, and infarct size (P<0.05 compared with ATV+$^{ATV-}$MSCs group) (**Figures 3**, **4**, S1). Inhibition of SDF-1/CXCR4 with AMD3100 also significantly abrogated the effects of the combination regimen

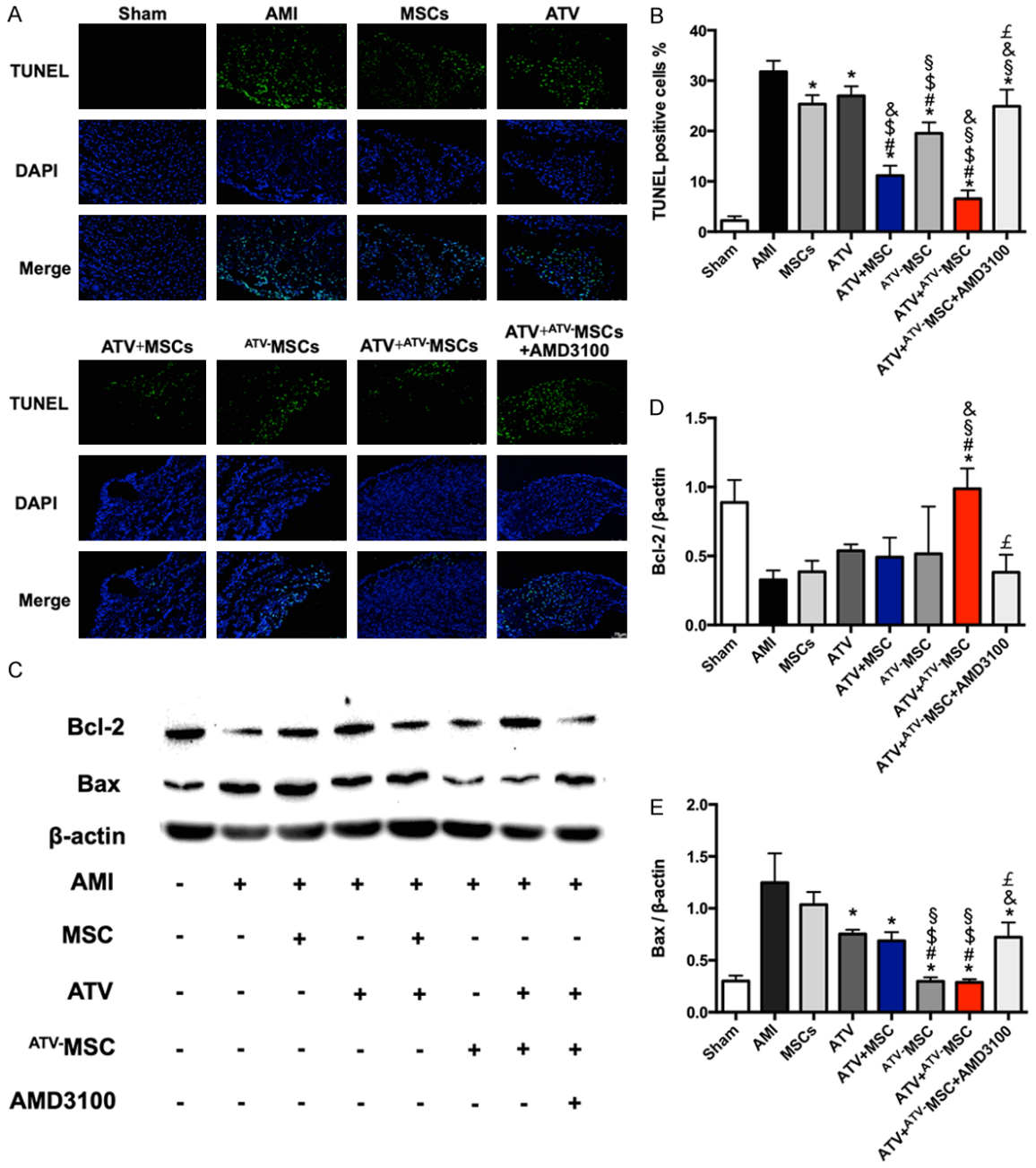

Figure 5. Apoptosis of cardiomyocytes were evaluated with TUNEL and western blot. A. Representative images of TUNEL staining in peri-infarct myocardium in each group (× 200). B. Ratio of apoptotic cells to total cells in each group. ATV+$^{ATV-}$MSCs exerted most potent anti-apoptotic effect when compared with MSCs only, which was almost completely abolished by AMD3100. C. Representative images of Bcl-2 and Bax expressions in peri-infarct myocardium assessed with western blot in each group. D. Quantitative data for the Bcl-2/β-actin in each group. E. Quantitative data for the Bax/β-actin in each group. Combined regimen of ATV and $^{ATV-}$MSCs significantly increased Bcl-2 expression, which was significantly reversed with the treatment of AMD3100. Bax expression was decreased in both ATV and ATV+MSCs treatment group compared with AMI control, which further decreased with the treatment of $^{ATV-}$MSCs and ATV+$^{ATV-}$MSCs. Compared with ATV+$^{ATV-}$MSCs group, the addition administration of AMD3100 significantly increased Bax expression. *P<0.05 compared with AMI group; #P<0.05 compared with MSCs group; $$P$<0.05 compared with ATV group; §P<0.05 compared with ATV+MSCs group; &P<0.05 compared with $^{ATV-}$MSCs group; £P<0.05 compared with ATV+$^{ATV-}$MSCs group. AMI: acute myocardial infarction; ATV: atorvastatin; MSCs: mesenchymal stem cells; $^{ATV-}$MSCs: atorvastatin pretreated mesenchymal stem cells; TUNEL: terminal-deoxynucleotidyltransferase-mediated dUTP nick end labeling; DAPI: 4'6-diamidino-2-phenylindole dihydrochloride. Scale bar = 75 μm.

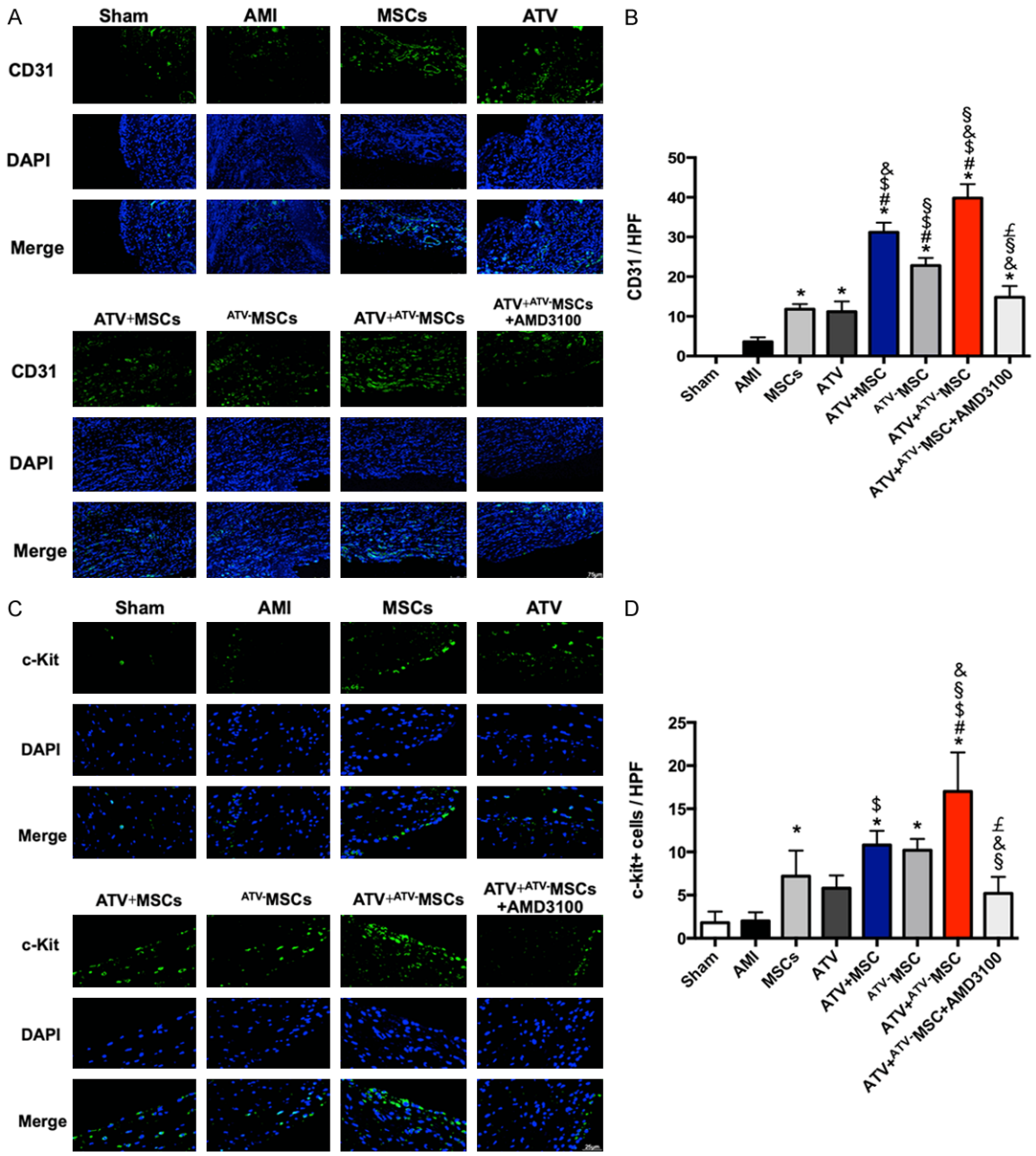

Figure 6. Angiogenesis in peri-infarct region was evaluated with CD31 staining. c-Kit$^+$ cells were assessed with immunofluorescence. (A) Representative images of CD31 staining in each group (× 200). (B) Angiogenesis was evaluated with number of CD31 positive vessels per HPF. ATV+$^{ATV-}$MSCs significantly enhanced CD31 positive vessels compared with $^{ATV-}$MSCs and ATV+MSCs groups, which was markedly reversed by AMD3100 treatment. (C) Representative images of c-Kit staining in each group (× 600). (D) Number of c-Kit$^+$ cells in the peri-infarct region per HPF. ATV+$^{ATV-}$MSCs group demonstrated a markedly significant increase in the number of c-Kit$^+$ cells compared with all other groups, which was abolished with the treatment of AMD3100. *P<0.05 compared with AMI group; #P<0.05 compared with MSCs group; $$P$<0.05 compared with ATV group; §P<0.05 compared with ATV+MSCs group; &P<0.05 compared with $^{ATV-}$MSCs group; £P<0.05 compared with ATV+$^{ATV-}$MSCs group. AMI: acute myocardial infarction; ATV: atorvastatin; MSCs: mesenchymal stem cells; $^{ATV-}$MSCs: atorvastatin pretreated mesenchymal stem cells; DAPI: 4'6-diamidino-2-phenylindole dihydrochloride; HPF: high power field. Scale bar = 75 μm (A), 25 μm (C).

on targeted recruitment and survival of MSCs, anti-inflammation, anti-apoptosis, pro-angiogenesis and arteriogenesis, and mobilization of c-Kit$^+$ cells (P<0.05) (**Figures 2**, **5**, **6**, S2), indicating that these cardioprotective effects conferred by ATV+$^{ATV-}$MSCs were mainly attributed to the augmented activation of SDF-1/CXCR4 pathway.

Discussion

The current study provides novel laboratory evidence extending the previous report by showing that a combination of statin and statin-preconditioned stem cells improves cardiac repair and regeneration. It has been shown that following the transplantation, majority of the transplanted stem cells fail to survive in the inflammatory microenvironment of an infarcted heart [24]. This low engraftment rate is believed to be the bottleneck of cell therapy that needs to be overcome for further improving the efficacy of stem cell therapy [9, 24-26]. Our previous studies demonstrated that high dose of oral ATV administration improved the survival of MSCs and heart function through ameliorating undesirable effects of cardiac infarction [15-17, 21, 27, 28]. Additionally, our prior studies also indicated that ATV-pretreated MSCs not only exerted anti-apoptotic effect but also improved targeted recruitment of MSCs by increasing the expression of CXCR4 on MSCs surface [21, 22]. Based on these studies, we reasoned that the combined oral administration of ATV with ^{ATV}MSCs transplantation could have a more enhanced therapeutic effect in a rat model of AMI. The main findings in the present study include that: 1) ATV treatment of rats with AMI extended the window of SDF-1 peak level of expression in the infarcted myocardium up to 1 week post-AMI; 2) ATV+^{ATV}MSCs transplantation remarkably enhanced the targeted recruitment and survival of transplanted MSCs accompanied by remarkable enhancement of heart functional recovery, attenuation of ventricular remodeling and infarct size reduction; 3) at the cellular level, cardiac functional improvement was mostly attributable to marked inhibition of inflammation and myocardial apoptosis, enhanced angiogenesis and mobilization of c-Kit$^+$ stem cells in the infarcted myocardium; 4) at the molecular level, the beneficial effects conferred by ATV+^{ATV}MSCs were mostly attributable to an augmented SDF-1/CXCR4 signaling activation.

SDF-1/CXCR4 signaling plays an important role in MSCs targeted recruitment, retention, and survival [29, 30]. Overexpressing SDF-1 using genetic approaches locally after ischemic insult resulted in striking enhancement in the migration and survival of transplanted MSCs [12, 31-33]. However, it remains a major obstacle to elevate SDF-1 expression in the infarcted hearts as manipulating SDF-1 expression with genetic approaches is currently clinically infeasible. On the other hand, the narrow window of SDF-1 upregulation, from day 1-3 post AMI [12, 34], not only provides insufficient time for the transplanted stem cells to be recruited to myocardial infarcted area [34], but also renders the recruited MSCs difficult to survive the intense inflammatory and oxidative environment in early stage infarcted myocardium [35].

Based on the results of previous studies that statins has anti-apoptosis, anti-inflammation and anti-oxidation effects [36, 37], we propose that ATV treatment could "fertilize the sterile soil" of harsh environment in the infarcted myocardium and improve the transplanted MSCs survival and cardiac performance in murine and porcine models of AMI [15-17, 28, 38, 39]. In this study, we provided evidence that ATV treatment could not only extend the peak level of SDF-1 expression in the peri-infarct region from day 1 to 1 week after infarction, but also maintained SDF-1 expression at a high level up to 2 week post AMI, thereby allowing us to transplant MSCs at desirable time point for an enhanced targeted recruitment and survival of the transplanted cells. More importantly, enhancing the expression of SDF-1 in the post-infarction heart by ATV treatment is clinically more feasible than the genetic approaches used in previous studies [12, 31-33].

Other than SDF-1, another key factor in the chemotactic SDF-1/CXCR4 signaling pathway is the receptor CXCR4 [10-13, 40]. Previous studies have shown that increasing CXCR4 expression improved the engraftment of MSCs [41, 42]. Consistent with these findings, our recent study revealed that ATV pretreated MSCs could not only have anti-apoptotic effect, but also enhanced CXCR4 expression on the cell surface of MSCs and promoted targeted recruitment of MSCs towards the injured myocardium, thereby resulting in improved cardiac performance [21, 22]. In this study, we further demonstrated that ATV+MSCs and ^{ATV}MSCs resulted in a respective 1.20 and 1.30 fold increases, and ATV+^{ATV}MSCs led to even a 2.4 fold increase in the recruitment and survival of the transplanted MSCs in the infarcted myocardium. These remarkable increases in the recruitment and survival of MSCs by ATV+^{ATV}MSCs

may result from an upregulation of SDF-1 expression, suppression of inflammation in the infarcted area [18, 43], and an augmentation of CXCR4 expression on the transplanted ^{ATV}MSCs surface [20-22].

Furthermore, the combination regimen presented in the current study exhibited striking enhancement of therapeutic effect, resulting in marked improvement of cardiac function (ΔLVEF: +15.8%), significant attenuation of adverse ventricular remodeling (ΔLVESd: -0.19 mm) and great reduction of infarct size by 42.4%. To the best of our knowledge, this is the first report of a clinically feasible strategy that greatly enhances the recruitment, survival and efficacy of transplanted MSCs. Thus, the combination regimen may represent a big breakthrough in stem cell therapy for AMI.

In addition, our study also revealed that the striking therapeutic benefits conferred by the synergistic effects of ATV and ^{ATV}MSCs are associated with anti-inflammation and anti-apoptosis activity, and enhancement of angiogenesis and c-Kit$^+$ stem cell mobilization. It was well documented that ATV by itself has anti-inflammatory and even immunomodulatory effects [44], and MSCs could also release anti-inflammatory cytokines, and reduce the number of natural killer cells and neutrophils in the post-infarct heart [2]. Consistent with these findings, we demonstrated in this study that MSCs or ATV treatment decreased the number of inflammatory cells and cytokines in infarcted and peri-infarct myocardium, while ATV+^{ATV}MSCs could further profoundly suppress infiltration of inflammatory cells and the production of pro-inflammatory cytokines of IL-1β, IL-6 and TNF-α, and additionally upregulate the expression of the anti-inflammatory cytokine IL-10. Both the anti-inflammatory effect afforded by ATV [15, 16, 43, 45] and the enhanced targeted MSCs recruitment by both ATV [18-20] and ^{ATV}MSCs [22] act synergistically to suppress inflammation, thereby promoting MSCs survival.

Consistent with our previous reports, this study demonstrated that ATV+MSCs and ^{ATV}MSCs treatments had greater anti-apoptotic effect than ATV and MSCs alone [15, 16]. More importantly, we found that ATV+^{ATV}MSCs was the most potent anti-apoptotic treatment that enhanced the survival of cardiomyocytes in peri-infarct region, which could in part led to their striking cardioprotective effects. MSCs have been shown to secret cytokines to suppress apoptosis and promote cardiomyocytes survival under ischemic insult [4]. Our previous studies showed that ATV treatment were anti-apoptotic [46], and the combined administration of ATV and MSCs further protected cardiomyocytes against apoptosis [15-17, 39]. Since ^{ATV}MSCs had greater anti-apoptotic activity [21] and exhibited enhanced targeted recruitment to infarct myocardium possibly due to the increased expression of CXCR4 on their cell surface [22], it is conceivable that the combined enhancement of anti-apoptotic effect and targeted recruitment of ^{ATV}MSCs could synergistically promote cardiomyocyte survival in the infarct heart, thereby reducing infarct size, and attenuating AMI-induced adverse structural remodeling and deterioration in LV function. To the best of our knowledge, similar finding has not been reported before.

In this study, we also found that ATV+^{ATV}MSCs treatment promoted angiogenesis in peri-infarct regions, which could further help to repair the damaged heart. The pro-angiogenesis effect of ATV is attributable to enhanced endothelial progenitor cells (EPC) targeted migration [47] into ischemic sites [19]. Since ATV treatment upregulated SDF-1 in ischemic cardiac tissues, the circulating CXCR4 positive stem cells [48] or the transplanted ^{ATV}MSCs with elevated CXCR4 [22] reported in current study could be more likely recruited to the injured heart to form new vessels. Additionally, a recent study indicated that MSCs employ the SDF-1/CXCR4 and SCF/c-Kit signaling pathways to promote migration and differentiation of endogenous stem cells [1]. In line with these studies, our data demonstrated that ATV+^{ATV}MSCs resulted in a 1.4 fold increase in c-Kit$^+$ cells recruitment, even though the combination protocol did not enhance MSCs' lineage commitment toward contractile cardiac myocytes.

Most importantly, our study demonstrated that the remarkable therapeutic effects of ATV+^{ATV}MSCs were almost completely abolished by the SDF-1/CXCR4 signaling antagonist AMD3100, suggesting that the SDF-1/CXCR4 signaling are the major signaling that mediates the effect of ATV+^{ATV}MSCs on enhancement of cardiac per-

formance. In conclusion, the combination regimen of oral administration of ATV with intravenous ^{ATV}MSCs transplantation can markedly enhance targeted recruitment, survival, and therapeutic efficacy of transplanted MSCs through augmented activation of SDF-1/CXCR4 pathway. Our study thus suggest ATV+^{ATV}MSCs combination regimen as a promising strategy for the further improvement of the clinical therapeutic efficacy of MSCs in patients with AMI.

Clinical perspectives

We have recently shown that the cholesterol lowering drugs, statins, improve stem cell capacity of cardiac tissue repair and regeneration. The current study extends the previous observations, and for the first time, demonstrates that the combined regimen of atorvastatin (ATV) and ATV-pretreated mesenchymal stem cells (^{ATV}MSCs) transplantation exhibits prominent augmentation of targeted recruitment and survival of transplanted MSCs, and improvement of cardiac function after AMI through augmented activation of SDF-1/CXCR4 axis. Thus, our study reveals the possibility that ATV combined with ^{ATV}MSCs may be a promising therapeutic strategy with potential clinical applications for treating AMI.

Acknowledgements

This work was supported by grants from CAMS Innovation Fund for Medical Sciences (CIFMS, 2016-12M-1-009), Innovative Research Foundation of Peking Union Medical College (2012-1002-31), 863 Program of China (2011AA0-20110) and National Natural Science Foundation of China (81700362, 81300112, 81170129, 81200107). We wish to thank Pei-He Wang and Fu-Liang Luo (Experimental Animal Center) for technical assistance.

Disclosure of conflict of interest

None.

Address correspondence to: Dr. Yue-Jin Yang, State Key Laboratory of Cardiovascular Disease, Fuwai Hospital, National Center for Cardiovascular Diseases, Chinese Academy of Medical Sciences and Peking Union Medical College, Fuwai Hospital, No. 167 Beilishi Road, Xicheng District, Beijing 100037, People's Republic of China. Tel: +86 10 88398760; Fax: +86 10 68351786; E-mail: yangyjfw@126.com

References

[1] Hatzistergos KE, Saur D, Seidler B, Balkan W, Breton M, Valasaki K, Takeuchi LM, Landin AM, Khan A and Hare JM. Stimulatory effects of mesenchymal stem cells on ckit+ cardiac stem cells are mediated by SDF1/CXCR4 and SCF/cKit signaling pathways. Circ Res 2016; 119: 921-930.

[2] Luger D, Lipinski MJ, Westman PC, Glover DK, Dimastromatteo J, Frias JC, Albelda MT, Sikora S, Kharazi A, Vertelov G, Waksman R and Epstein SE. Intravenously delivered mesenchymal stem cells: systemic anti-inflammatory effects improve left ventricular dysfunction in acute myocardial infarction and ischemic cardiomyopathy. Circ Res 2017; 120: 1598-1613.

[3] Taylor DA, Chandler AM, Gobin AS and Sampaio LC. Maximizing cardiac repair: should we focus on the cells or on the matrix? Circ Res 2017; 120: 30-32.

[4] Shafei AE, Ali MA, Ghanem HG, Shehata AI, Abdelgawad AA, Handal HR, Talaat KA, Ashaal AE and El-Shal AS. Mesenchymal stem cell therapy: a promising cell-based therapy for treatment of myocardial infarction. J Gene Med 2017; 19: e2995.

[5] Williams AR and Hare JM. Mesenchymal stem cells: biology, pathophysiology, translational findings, and therapeutic implications for cardiac disease. Circ Res 2011; 109: 923-940.

[6] Liu B, Duan CY, Luo CF, Ou CW, Sun K, Wu ZY, Huang H, Cheng CF, Li YP and Chen MS. Effectiveness and safety of selected bone marrow stem cells on left ventricular function in patients with acute myocardial infarction: a meta-analysis of randomized controlled trials. Int J Cardiol 2014; 177: 764-70.

[7] Afzal MR, Samanta A, Shah ZI, Jeevanantham V, Abdel-Latif A, Zuba-Surma EK and Dawn B. Adult bone marrow cell therapy for ischemic heart disease: evidence and insights from randomized controlled trials. Circ Res 2015; 117: 558-575.

[8] Hu X, Xu Y, Zhong Z, Wu Y, Zhao J, Wang Y, Cheng H, Kong M, Zhang F, Chen Q, Sun J, Li Q, Jin J, Li Q, Chen L, Wang C, Zhan H, Fan Y, Yang Q, Yu L, Wu R, Liang J, Zhu J, Wang Y, Jin Y, Lin Y, Yang F, Jia L, Zhu W, Chen J, Yu H, Zhang J and Wang J. A large-scale investigation of hypoxia-preconditioned allogeneic mesenchymal stem cells for myocardial repair in nonhuman primates: paracrine activity without remuscularization. Circ Res 2016; 118: 970-983.

[9] Sanganalmath SK and Bolli R. Cell therapy for heart failure: a comprehensive overview of experimental and clinical studies, current challenges, and future directions. Circ Res 2013; 113: 810-834.

[10] Dong F, Harvey J, Finan A, Weber K, Agarwal U and Penn MS. Myocardial CXCR4 expression is required for mesenchymal stem cell mediated repair following acute myocardial infarction. Circulation 2012; 126: 314-324.
[11] Zaruba MM and Franz WM. Role of the SDF-1-CXCR4 axis in stem cell-based therapies for ischemic cardiomyopathy. Expert Opin Biol Ther 2010; 10: 321-335.
[12] Mayorga ME, Kiedrowski M, McCallinhart P, Forudi F, Ockunzzi J, Weber K, Chilian W, Penn MS and Dong F. Role of SDF-1: CXCR4 in impaired post-myocardial infarction cardiac repair in diabetes. Stem Cells Transl Med 2018; 7: 115-124.
[13] Li J, Guo W, Xiong M, Han H, Chen J, Mao D, Tang B, Yu H and Zeng Y. Effect of SDF-1/CXCR4 axis on the migration of transplanted bone mesenchymal stem cells mobilized by erythropoietin toward lesion sites following spinal cord injury. Int J Mol Med 2015; 36: 1205-1214.
[14] Hajinejad M, Pasbakhsh P, Omidi A, Mortezaee K, Nekoonam S, Mahmoudi R and Kashani IR. Resveratrol pretreatment enhanced homing of SDF-1alpha-preconditioned bone marrow-derived mesenchymal stem cells in a rat model of liver cirrhosis. J Cell Biochem 2018; 119: 2939-2950.
[15] Yang YJ, Qian HY, Huang J, Geng YJ, Gao RL, Dou KF, Yang GS, Li JJ, Shen R, He ZX, Lu MJ and Zhao SH. Atorvastatin treatment improves survival and effects of implanted mesenchymal stem cells in post-infarct swine hearts. Eur Heart J 2008; 29: 1578-1590.
[16] Yang YJ, Qian HY, Huang J, Li JJ, Gao RL, Dou KF, Yang GS, Willerson JT and Geng YJ. Combined therapy with simvastatin and bone marrow-derived mesenchymal stem cells increases benefits in infarcted swine hearts. Arterioscler Thromb Vasc Biol 2009; 29: 2076-2082.
[17] Zhang Q, Wang H, Yang YJ, Dong QT, Wang TJ, Qian HY, Li N, Wang XM and Jin C. Atorvastatin treatment improves the effects of mesenchymal stem cell transplantation on acute myocardial infarction: the role of the RhoA/ROCK/ERK pathway. Int J Cardiol 2014; 176: 670-679.
[18] Qiu R, Cai A, Dong Y, Zhou Y, Yu D, Huang Y, Zheng D, Rao S, Feng Y and Mai W. SDF-1alpha upregulation by atorvastatin in rats with acute myocardial infarction via nitric oxide production confers anti-inflammatory and anti-apoptotic effects. J Biomed Sci 2012; 19: 99.
[19] Chiang KH, Cheng WL, Shih CM, Lin YW, Tsao NW, Kao YT, Lin CT, Wu SC, Huang CY and Lin FY. Statins, HMG-CoA reductase inhibitors, improve neovascularization by increasing the expression density of CXCR4 in endothelial progenitor cells. PLoS One 2015; 10: e0136405.
[20] Cai A, Qiu R, Li L, Zheng D, Dong Y, Yu D, Huang Y, Rao S, Zhou Y and Mai W. Atorvastatin treatment of rats with ischemia-reperfusion injury improves adipose-derived mesenchymal stem cell migration and survival via the SDF-1alpha/CXCR-4 axis. PLoS One 2013; 8: e79100.
[21] Dong Q, Yang Y, Song L, Qian H and Xu Z. Atorvastatin prevents mesenchymal stem cells from hypoxia and serum-free injury through activating AMP-activated protein kinase. Int J Cardiol 2011; 153: 311-316.
[22] Li N, Yang YJ, Qian HY, Li Q, Zhang Q, Li XD, Dong QT, Xu H, Song L and Zhang H. Intravenous administration of atorvastatin-pretreated mesenchymal stem cells improves cardiac performance after acute myocardial infarction: role of CXCR4. Am J Transl Res 2015; 7: 1058-1070.
[23] Cavasin MA, Tao Z, Menon S and Yang XP. Gender differences in cardiac function during early remodeling after acute myocardial infarction in mice. Life Sci 2004; 75: 2181-2192.
[24] Segers VF and Lee RT. Stem-cell therapy for cardiac disease. Nature 2008; 451: 937-942.
[25] Hofmann M, Wollert KC, Meyer GP, Menke A, Arseniev L, Hertenstein B, Ganser A, Knapp WH and Drexler H. Monitoring of bone marrow cell homing into the infarcted human myocardium. Circulation 2005; 111: 2198-2202.
[26] Geng YJ. Molecular mechanisms for cardiovascular stem cell apoptosis and growth in the hearts with atherosclerotic coronary disease and ischemic heart failure. Ann N Y Acad Sci 2003; 1010: 687-697.
[27] Li N, Zhang Q, Qian H, Jin C, Yang Y and Gao R. Atorvastatin induces autophagy of mesenchymal stem cells under hypoxia and serum deprivation conditions by activating the mitogen-activated protein kinase/extracellular signal-regulated kinase pathway. Chin Med J (Engl) 2014; 127: 1046-1051.
[28] Song L, Yang YJ, Dong QT, Qian HY, Gao RL, Qiao SB, Shen R, He ZX, Lu MJ, Zhao SH, Geng YJ and Gersh BJ. Atorvastatin enhance efficacy of mesenchymal stem cells treatment for swine myocardial infarction via activation of nitric oxide synthase. PLoS One 2013; 8: e65702.
[29] Marquez-Curtis LA and Janowska-Wieczorek A. Enhancing the migration ability of mesenchymal stromal cells by targeting the SDF-1/CXCR4 axis. Biomed Res Int 2013; 2013: 561098.
[30] Wen J, Zhang JQ, Huang W and Wang Y. SDF-1alpha and CXCR4 as therapeutic targets in cardiovascular disease. Am J Cardiovasc Dis 2012; 2: 20-28.
[31] Tilokee EL, Latham N, Jackson R, Mayfield AE, Ye B, Mount S, Lam BK, Suuronen EJ, Ruel M, Stewart DJ and Davis DR. Paracrine engineer-

ing of human explant-derived cardiac stem cells to over-express stromal-cell derived factor 1alpha enhances myocardial repair. Stem Cells 2016; 34: 1826-1835.
[32] Askari AT, Unzek S, Popovic ZB, Goldman CK, Forudi F, Kiedrowski M, Rovner A, Ellis SG, Thomas JD, DiCorleto PE, Topol EJ and Penn MS. Effect of stromal-cell-derived factor 1 on stem-cell homing and tissue regeneration in ischaemic cardiomyopathy. Lancet 2003; 362: 697-703.
[33] Zhang M, Mal N, Kiedrowski M, Chacko M, Askari AT, Popovic ZB, Koc ON and Penn MS. SDF-1 expression by mesenchymal stem cells results in trophic support of cardiac myocytes after myocardial infarction. FASEB J 2007; 21: 3197-3207.
[34] Ma J, Ge J, Zhang S, Sun A, Shen J, Chen L, Wang K and Zou Y. Time course of myocardial stromal cell-derived factor 1 expression and beneficial effects of intravenously administered bone marrow stem cells in rats with experimental myocardial infarction. Basic Res Cardiol 2005; 100: 217-223.
[35] Chen Y, Teng X, Chen W, Yang J, Yang Z, Yu Y and Shen Z. Timing of transplantation of autologous bone marrow derived mesenchymal stem cells for treating myocardial infarction. Sci China Life Sci 2014; 57: 195-200.
[36] Liao JK and Laufs U. Pleiotropic effects of statins. Annu Rev Pharmacol Toxicol 2005; 45: 89-118.
[37] Wassmann S, Laufs U, Muller K, Konkol C, Ahlbory K, Baumer AT, Linz W, Bohm M and Nickenig G. Cellular antioxidant effects of atorvastatin in vitro and in vivo. Arterioscler Thromb Vasc Biol 2002; 22: 300-305.
[38] Song L, Yang YJ, Dong QT, Qian HY, Xu H, Meng XM and Tang Y. Atorvastatin protects swine bone marrow mesenchymal stem cells from apoptosis through AMPK but not PI3K/Akt pathway. Zhonghua Xin Xue Guan Bing Za Zhi 2011; 39: 1033-1038.
[39] Xu H, Yang YJ, Qian HY, Tang YD, Wang H and Zhang Q. Rosuvastatin treatment activates JAK-STAT pathway and increases efficacy of allogeneic mesenchymal stem cell transplantation in infarcted hearts. Circ J 2011; 75: 1476-1485.
[40] Yang D, Sun S, Wang Z, Zhu P, Yang Z and Zhang B. Stromal cell-derived factor-1 receptor CXCR4-overexpressing bone marrow mesenchymal stem cells accelerate wound healing by migrating into skin injury areas. Cell Reprogram 2013; 15: 206-215.
[41] Xie J, Wang H, Song T, Wang Z, Li F, Ma J, Chen J, Nan Y, Yi H and Wang W. Tanshinone IIA and astragaloside IV promote the migration of mesenchymal stem cells by up-regulation of CXCR4. Protoplasma 2013; 250: 521-530.
[42] Zhang D, Fan GC, Zhou X, Zhao T, Pasha Z, Xu M, Zhu Y, Ashraf M and Wang Y. Over-expression of CXCR4 on mesenchymal stem cells augments myoangiogenesis in the infarcted myocardium. J Mol Cell Cardiol 2008; 44: 281-292.
[43] Hu X, Sun A, Xie X, Huang Z, Jia J, Yao R and Ge J. Rosuvastatin changes cytokine expressions in ischemic territory and preserves heart function after acute myocardial infarction in rats. J Cardiovasc Pharmacol Ther 2013; 18: 162-176.
[44] Xu X, Gao W, Cheng S, Yin D, Li F, Wu Y, Sun D, Zhou S, Wang D, Zhang Y, Jiang R and Zhang J. Anti-inflammatory and immunomodulatory mechanisms of atorvastatin in a murine model of traumatic brain injury. J Neuroinflammation 2017; 14: 167.
[45] Cui X, Chopp M, Zacharek A, Roberts C, Lu M, Savant-Bhonsale S and Chen J. Chemokine, vascular and therapeutic effects of combination simvastatin and BMSC treatment of stroke. Neurobiol Dis 2009; 36: 35-41.
[46] Li Q, Dong QT, Yang YJ, Tian XQ, Jin C, Huang PS, Jiang LP and Chen GH. AMPK-mediated cardioprotection of atorvastatin relates to the reduction of apoptosis and activation of autophagy in infarcted rat hearts. Am J Transl Res 2016; 8: 4160-4171.
[47] Wang D, Li T, Wei H, Wang Y, Yang G, Tian Y, Zhao Z, Wang L, Yu S, Zhang Y, Chen J, Jiang R and Zhang JN. Atorvastatin enhances angiogenesis to reduce subdural hematoma in a rat model. J Neurol Sci 2016; 362: 91-99.
[48] Yamaguchi J, Kusano KF, Masuo O, Kawamoto A, Silver M, Murasawa S, Bosch-Marce M, Masuda H, Losordo DW, Isner JM and Asahara T. Stromal cell-derived factor-1 effects on ex vivo expanded endothelial progenitor cell recruitment for ischemic neovascularization. Circulation 2003; 107: 1322-1328.

Table S1. Changes of SDF-1 expression in peri-infarcted region during the time course assessed with IHC, ELISA and PCR

	IHC (%)			ELISA (pg/mg)			RT-PCR		
	d1	d7	d14	d1	d7	d14	d1	d7	d14
Sham	0.458±0.146	0.468±0.159	0.288±0.094	28.56±3.315	28.84±3.809	27.62±4.725	0.994±0.094	0.784±0.256	0.828±0.125
AMI	3.598±0.573	1.916±0.425	1.17±0.300	50.02±2.868	40.00±6.954	31.32±1.564	2.166±0.640	1.222±0.232	1.034±0.316
ATV	3.596±0.561	4.052±0.726*	2.642±0.183*	51.24±7.453	61.26±7.617*	44.34±4.043*	2.258±0.179	2.036±0.497*	1.336±0.325

IHC (Immunohistochemistry), ELISA (Enzyme Lined Immunosorbent Assay), RT-PCR (real time polymerase chain reaction). d1, d7, d14 refers to the 1st, 7th and 14th day post AMI. *P<0.05 compared with AMI group at the corresponding day.

Table S2. Cardiac function evaluated by left heart catheterization at endpoint

	LVEDP (mmHg)	dp/dt (mmHg/s)	-dp/dt (mmHg/s)
Sham	3.49±0.6	4935.68±295.28	3855.26±415.46
AMI	29.17±2.44	3321.22±262.24	2935.31±186.80
MSCs	24.79±1.18*	3469.25±141.91	3313.04±129.72*
ATV	23.42±1.95*	3677.67±102.09*	3313.68±98.42*
ATV+MSCs	14.69±1.87*,#,$,&	4291.09±209.97*,#,$	3542.56±233.71*
$^{ATV-}$MSCs	17.46±2.7*,#,$	4085.91±258.97*,#,$	3513.44±190.18*
ATV+$^{ATV-}$MSCs	10.61±1.49*,#,$,§,&	4676.05±219.76*,#,$,§,&	3745.19±154.53*,#,$
ATV+$^{ATV-}$MSCs+AMD3100	24.64±1.99*,§,&,£	3480.76±111.65§,£	3162.71±275.3§,&,£

LVEDP (left ventricular end-diastolic dimension), dp/dtmax (left ventricular pressure maximal rate of rise), -dp/dtmax (left ventricular pressure maximal rate of fall) detected at endpoint (4 weeks post AMI), respectively. n = 10 in each group. *P<0.05 compared with AMI group; #P<0.05 compared with MSCs group; $$P$<0.05 compared with ATV group; §P<0.05 compared with ATV+MSCs group; &P<0.05 compared with $^{ATV-}$MSCs group; £P<0.05 compared with ATV+$^{ATV-}$MSCs group.

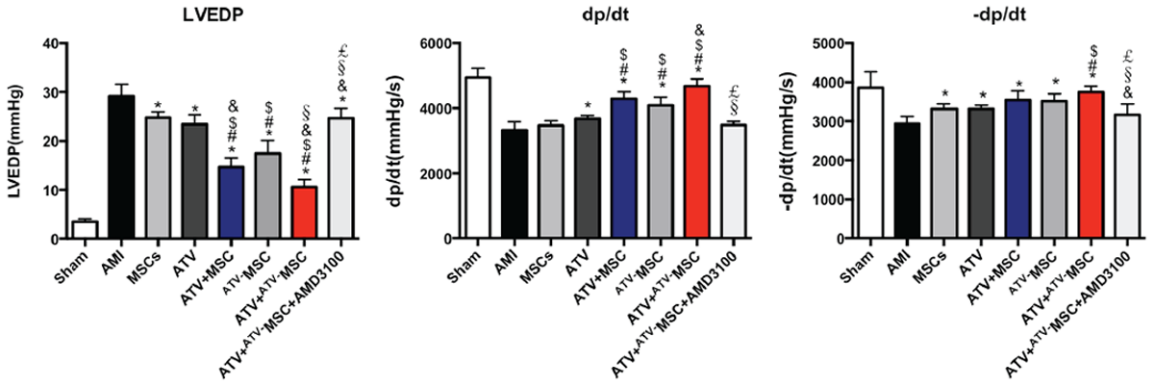

Figure S1. Left heart catheterization assessment of cardiac function. The values of LVEDP (left ventricular end-diastolic dimension), dp/dtmax (left ventricular pressure maximal rate of rise) and -dp/dtmax (left ventricular pressure maximal rate of fall) detected at endpoint (4 weeks post AMI), respectively. n = 10 in each group. *P<0.05 compared with AMI group; #P<0.05 compared with MSCs group; $$P$<0.05 compared with ATV group; §P<0.05 compared with ATV+MSCs group; &P<0.05 compared with $^{ATV-}$MSCs group; £P<0.05 compared with ATV+$^{ATV-}$MSCs group.

Table S3. Quantitation of infarct area, neutrophil infiltration and measurement of IL-1β, IL-6, TNF-α, IL-10 expressions in the peri-infarcted myocardium

	Infarct area/ LV (%)	NE/mm^2	IL-1β	IL-6	TNF-α	IL-10
Sham	0.89±1.23	48.40±10.09	104.3±36.50	1987±187.9	62.33±16.01	243.3±48.01
AMI	38.01±5.08	459.6±25.70	958.0±21.07	8514±144.4	885.7±25.11	741.3±21.59
MSCs	27.90±1.88*	373.6±25.6*	855.3±29.50*	7709±176.7*	796.7±16.01*	801.0±51.22
ATV	25.82±2.42*	353.2±30.81*	794.6±10.37*	7486±159.2*	713.3±24.01$^{*,\#}$	792.7±46.93
ATV+MSCs	19.71±2.86$^{*,\#,\$}$	293.6±29.79$^{*,\#,\$}$	731.0±20.52$^{*,\#,\$}$	6166±161.0$^{*,\#,\$}$	616.7±21.83$^{*,\#,\$}$	829.7±44.79
^{ATV}MSCs	20.28±2.38$^{*,\#,\$}$	306.8±36.69$^{*,\#,\$}$	772.3±20.11$^{*,\#,\$}$	6514±268.6$^{*,\#,\$}$	645.0±24.58$^{*,\#,\$}$	812.0±29.46
ATV+^{ATV}MSCs	16.06±2.32$^{*,\#,\$,\&}$	195.8±13.03$^{*,\#,\$,\S,\&}$	669.7±17.21$^{*,\#,\$,\S,\&}$	5591±206.6$^{*,\#,\$,\S,\&}$	596.3±16.65$^{*,\#,\$}$	870.0±22.65*
ATV+^{ATV}MSCs+AMD3100	30.51±2.84$^{*,\$,\&}$	422.6±34.66$^{\$,\S,\&,£}$	846.3±17.04$^{*,\S,\&,£}$	7562±92.634$^{*,\S,\&,£}$	779.3±20.43$^{*,\$,\S,\&,£}$	765.3±31.56

NE (neutrophils), IL (interleukin), TNF (tumor necrosis factor). n = 10 in each group. $^{*}P$<0.05 compared with AMI group; $^{\#}P$<0.05 compared with MSCs group; $^{\$}P$<0.05 compared with ATV group; $^{\S}P$<0.05 compared with ATV+MSCs group; $^{\&}P$<0.05 compared with ^{ATV}MSCs group; $^{£}P$<0.05 compared with ATV+^{ATV}MSCs group.

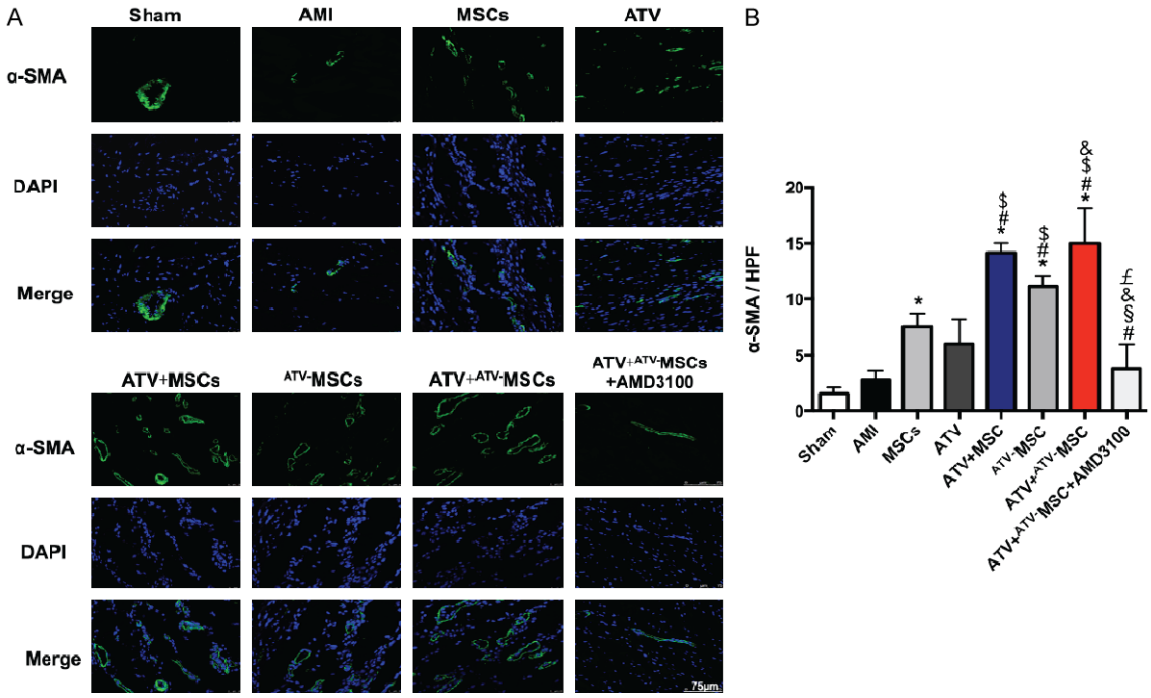

Figure S2. Arteriogenesis in peri-infarcted region was evaluated with α-SMA staining. A. Representative images of α-SMA staining in each group (× 400). B. Arteriogenesis was evaluated with number of α-SMA positive vessels per HPF. ATV+^{ATV}MSCs significantly enhanced α-SMA positive vessels compared with ^{ATV}MSCs group, which was markedly reversed by AMD3100 treatment. $^{*}P$<0.05 compared with AMI group; $^{\#}P$<0.05 compared with MSCs group; $^{\$}P$<0.05 compared with ATV group; $^{\S}P$<0.05 compared with ATV+MSCs group; $^{\&}P$<0.05 compared with ^{ATV}MSCs group; $^{£}P$<0.05 compared with ATV+^{ATV}MSCs group. AMI: acute myocardial infarction; ATV: atorvastatin; MSCs: mesenchymal stem cells; ^{ATV}MSCs: atorvastatin pretreated mesenchymal stem cells; DAPI: 4'6-diamidino-2-phenylindole dihydrochloride; α-SMA: α-smooth muscle actin; HPF: high power field. Scale bar = 75 μm.

Table S4. Quantitation of CM-DiI-labeled cells, apoptosis of cardiomyocytes, angiogenesis and c-Kit$^+$ cells in the peri-infarcted myocardium

	CM-DiI$^+$/DAPI (%)	TUNEL$^+$/DAPI (%)	α-SMA$^+$/HPF	CD31$^+$/HPF	c-Kit$^+$/HPF
Sham	-	2.22±0.86	1.60±0.55	2.20±0.84	1.80±1.30
AMI	-	31.78±2.18	2.80±0.84	3.60±1.14*	2.00±1.00
MSCs	7.70±2.31	25.33±1.77*	7.60±1.14*	11.80±1.30*	7.20±2.95*
ATV	-	26.98±1.89*	6.00±2.24	11.20±2.59*	5.80±1.48
ATV+MSCs	17.09±4.10$^{\#}$	11.17±1.94$^{*,\#,\$,\&}$	14.20±0.84$^{*,\#,\$}$	31.20±2.39$^{*,\#,\$,\&}$	10.80±1.64$^{*,\$}$
^{ATV}MSCs	17.67±4.37$^{\#}$	19.53±2.17$^{*,\#,\$,\S}$	11.20±0.84$^{*,\#,\$}$	22.80±1.92$^{*,\#,\$,\S}$	10.20±1.30*
ATV+^{ATV}MSCs	26.54±9.94$^{\#,\S,\&}$	6.57±1.67$^{*,\#,\$,\S,\&}$	15.00±3.16$^{*,\#,\$,\&}$	39.80±3.49$^{*,\#,\$,\S,\&}$	17.00±4.53$^{*,\#,\$,\S,\&}$
ATV+^{ATV}MSCs+AMD3100	8.85±2.78$^{£}$	24.91±3.32$^{*,\S,\&,£}$	3.80±2.17$^{\#,\S,\&,£}$	14.80±2.86$^{*,\S,\&,£}$	5.20±1.92$^{\S,\&,£}$

CM-DiI (1,1'-dioctadecyl-3,3,3',3'-tetramethylindocarbocyanine perchlorate), DAPI (4'6-diamidino-2-phenylindole dihydrochloride), TUNEL (terminal-deoxynucleotidyl transferase-mediated dUTP nick end labeling), HPF (high power field), α-SMA (α-smooth muscle actin). $^{*}P$<0.05 compared with AMI group; $^{\#}P$<0.05 compared with MSCs group; $^{\$}P$<0.05 compared with ATV group; $^{\S}P$<0.05 compared with ATV+MSCs group; $^{\&}P$<0.05 compared with ^{ATV}MSCs group; $^{£}P$<0.05 compared with ATV+^{ATV}MSCs group.

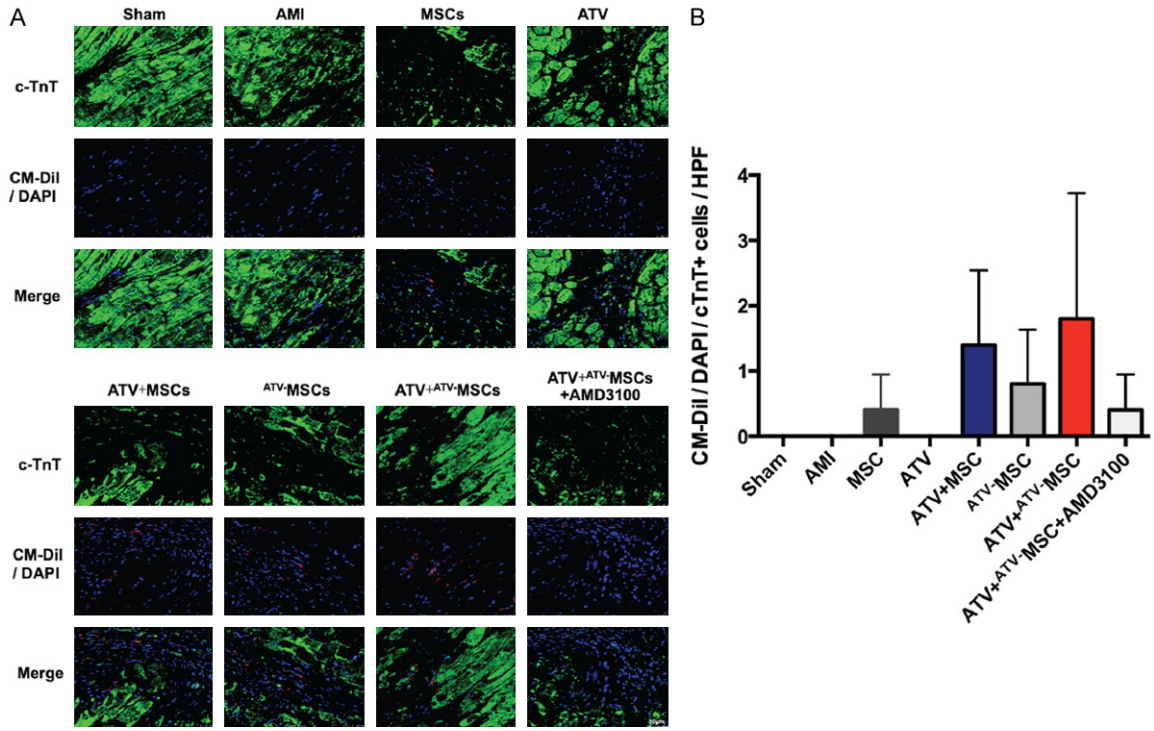

Figure S3. The differentiation of MSCs was evaluated with immunofluorescence. A. Representative images of cTnT staining in each group (× 400). B. Differentiation of MSCs into cardiomyocytes was evaluated with immunofluorescence of cTnT per HPF. AMI: acute myocardial infarction; ATV: atorvastatin; MSCs: mesenchymal stem cells; ^{ATV}MSCs: atorvastatin pretreated mesenchymal stem cells; DAPI: 4'6-diamidino-2-phenylindole dihydrochloride; c-TnT: cardiac troponin T; HPF: high power field. Scale bar = 50 μm.